

## Free energy of static quarks and the renormalized Polyakov loop in full QCD

---

**Konstantin Petrov\*, RBC-Bielefeld collaboration**

*NIC, DESY Zeuthen, Platanenallee 6, 15738 Zeuthen, Germany*

*E-mail: Konstantin.Petrov@desy.de*

We present results from a detailed study of singlet free energies in full QCD with realistic quark masses. An improved scheme for the non-perturbative renormalization of the Polyakov loop is used and we compare its temperature dependence for QCD with different flavor content. We also analyze screening masses extracted from singlet free energies at various temperatures close to and above the QCD transition temperature. We conclude that the temperature dependence of screening masses is well described by perturbation theory up to a non-perturbative pre-factor. An effective running coupling has been determined for all temperature values giving additional insight into screening phenomena at high temperature.

*The XXV International Symposium on Lattice Field Theory*

*July 30-4 August 2007*

*Regensburg, Germany*

---

\*Speaker.

## 1. Introduction

One of the most important properties of the quark gluon plasma is the screening of color charges [1]. It is expected that quarkonium states are dissociated due to screening of the color charges at temperatures somewhat higher than the deconfinement temperature. Moreover, Matsui and Satz conjectured [2] that quarkonium suppression can be viewed as a signature for the formation of a Quark-Gluon Plasma (QGP). While a calculation of spectral functions is best suited to study this phenomenon, their reliable calculation at finite temperature turns out to be quite difficult (see e.g. [3]). We present here a non-perturbative study of the screening of heavy quark-anti-quark interactions at finite temperature which is based on an analysis of the free energy of a static quark anti-quark pair [1]. Results for the free energy and its derivatives, the internal energy and entropy, can be used as input to potential model calculations, see e.g.[4, 5]. Furthermore, the study of static free energies is interesting as it allows for a non-perturbative renormalization of Polyakov loops. While the latter is not an order parameter in the presence of dynamical quarks it shows rapid variation in the transition region and therefore is widely used to describe the transition (crossover) in full QCD, e.g. through effective mean-field theories.

## 2. Numerical Analysis

This work is based on our large-scale finite temperature lattice calculations in (2+1)-flavor QCD in the region of small quark masses [6]. Our simulation have been performed with a physical strange quark mass and degenerate light quark masses,  $m_q = 0.1m_s$  ( $m_s$  being the strange quark mass), which correspond to a light pseudo-scalar mass  $m_\pi \simeq 220\text{MeV}$ . Lattice sizes vary between  $16^3 \times 4$  and  $24^3 \times 6$  lattices which correspond to the same physical volume. The lattice spacing and thus the temperature scale has been fixed using the Sommer scale  $r_0 = 0.469\text{ fm}$  [7]. For every value of the finite temperature coupling constant we performed corresponding zero temperature simulations where we extracted the zero temperature static quark potential. This has been used to set the temperature scale and to determine the renormalization constants used for a renormalization of the finite temperature free energies.

In our simulations we used the exact RHMC algorithm for simulations of (2+1)-flavor QCD. Further details about our simulations can be found in Refs.[6, 8]. On a large set of gauge field configurations, which are separated by 10 trajectories, we have calculated the singlet free energy,  $F_1(r, T)$ , of a static quark anti-quark pair. The singlet free energy, as well as the zero temperature static potential, are defined up to an additive constant  $C$ . Using temporal Wilson lines  $W(\vec{r})$  we write the former as

$$\exp(-F_1(r, T)/T + C) = \frac{1}{3} \langle \text{Tr} W(\vec{r}) W^\dagger(0) \rangle, \quad C = 2N_\tau \ln(Z_R). \quad (2.1)$$

The zero temperature potential is calculated from smeared Wilson loops  $W(r, \tau)$ ,

$$V_{(T=0)}(r) = - \lim_{\tau \rightarrow \infty} \ln \left( Z_R(\beta)^2 \frac{W(r, \tau)}{W(r, \tau + 1)} \right). \quad (2.2)$$

Here  $Z_R$  is zero temperature renormalization constant. Some details of our Wilson loop calculations are discussed in [8]. The above definition of a singlet free energy requires gauge fixing. For all

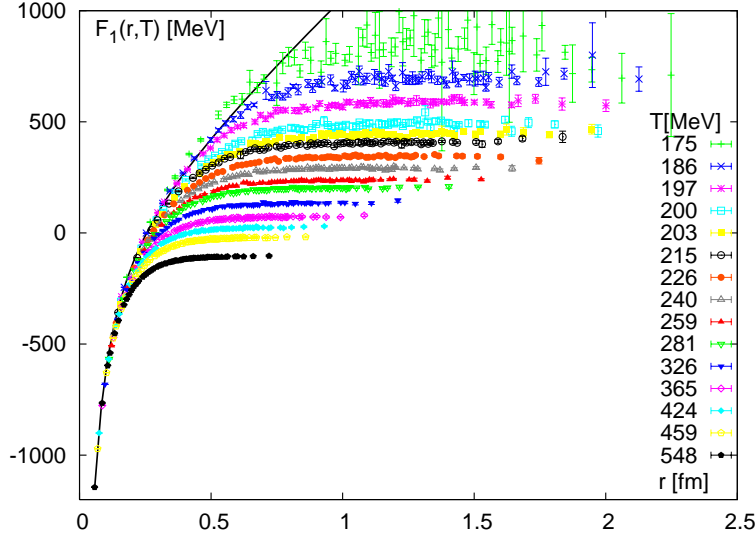


**Figure 1:** The singlet free energy calculated in  $(2+1)$ -flavor QCD on  $24^3 \times 6$  lattices at various temperatures. The solid line shows a fit to the zero temperature potential.

our calculations we use Coulomb gauge as it is done also in many previous closely related studies [9, 10, 11, 12, 13, 14]. In the zero temperature limit the singlet free energy coincides with the well-known static potential and, in fact, an analysis in a fixed gauge has been used also in this limit to calculate it [15]. At finite temperature  $F_1(r, T)$  characterizes the in-medium modification of inter-quark forces and color screening.

The renormalization constant  $Z_R$  introduced in Eq.2.2 is determined by matching result for the zero temperature static potential to the string potential,  $V_{string}(r) = -\pi/12r + \sigma r$ , at distance  $1.5r_0$ . Renormalizing the potentials at one point makes results obtained for a wide range of cut-off values coincide quite well at all distances [6]. Unlike in our earlier work, where we renormalized potentials at a short distance point, we now do so at a larger distance,  $r = 1.5r_0$ . This has the advantage that we can use the same large distance string potential,  $V_{string}(r)$ , for all our potentials, irrespective of the flavor content used in the simulation. At short distances this would not be the case as the running of the coupling entering the Coulomb term of the potential is sensitive to the number of flavors [6]. Of course, it also is important to note that we now have sufficient statistics to perform a reliable matching of potentials at the relatively large distance  $r = 1.5r_0$ . This also has the advantage that lattice-induced short-distance artifacts are significantly reduced in our analysis.

In Fig. 1 we show the singlet free energy calculated in  $(2+1)$ -flavor QCD on  $24^3 \times 6$  lattices together with the  $T = 0$  static potential. As one can see from the figure,  $F_1(r, T)$  is temperature independent at small distances and coincides with the zero temperature potential as expected. At large distances the singlet free energy approaches a constant value. This can be related to string breaking at low temperature and color screening at high temperatures. Note that the distance at which the free energy effectively flattens off is decreasing with increasing temperature. This is another indication for color screening at high temperature.

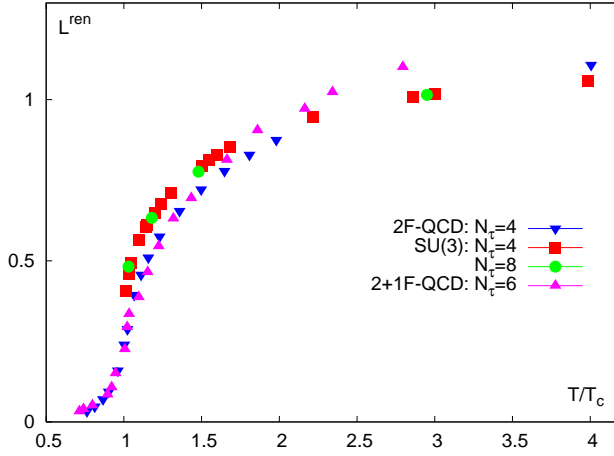


**Figure 2:** The renormalized Polyakov Loop calculated in  $(2+1)$ -flavor QCD on  $16^3 \times 4$  and  $24^3 \times 6$  lattices for different quark masses along a line of constant physics. Also shown in the figure are corresponding result from calculations in 2-flavor QCD and the SU(3) gauge theory.

### 3. Renormalized Polyakov Loop

The expectation value of the Polyakov loop  $\langle L(\vec{r}) \rangle = \langle \text{Tr} W(\vec{r}) \rangle$  is the order parameter for deconfinement in pure gauge theories. In full QCD there is no local order parameter because dynamical quarks break the relevant  $Z(3)$  symmetry explicitly. Still it remains an interesting quantity that can be used to analyze deconfinement in QCD as it shows a rapid increase in the crossover region [8, 16, 17] and can be used to determine the transition temperature [8, 17]. The Polyakov loop defined above strongly depends on the lattice spacing and requires renormalization. The singlet free energy and the Polyakov loop correlator, which defines the color averaged free energy, satisfy the cluster decomposition

$$\lim_{r \rightarrow \infty} \exp(-F_1(r, T) + C) = \frac{1}{9} \lim_{r \rightarrow \infty} \langle L(\vec{r}) L^\dagger(0) \rangle = |\langle L(0) \rangle|^2 \equiv L^2. \quad (3.1)$$

The normalization constant in the above expression is fixed through the renormalization of the zero temperature potential as discussed in the previous section. Thus, at large distances color averaged and singlet free energies approach the same constant,  $F_\infty(T)$ . We defined the renormalized Polyakov loop as

$$L^{\text{ren}}(T) = \exp\left(-\frac{F_\infty(T)}{2T}\right), \quad (3.2)$$

which due to the cluster decomposition is the same as

$$L^{\text{ren}}(T) = (Z_R(g^2))^{N_\tau} L. \quad (3.3)$$

Here the renormalization constants are the same as in Eq.2.2. Our numerical results for  $L^{\text{ren}}(T)$  obtained in simulations with different number of light quark flavors (two-flavour and pure gauge see [14]) and different lattice spacings are summarized in Fig.2. One can see from that figure that  $L^{\text{ren}}(T)$  shows an almost universal behavior as function of  $T/T_c$  for all quark masses studied by us, including the 2-flavor simulation. This suggests, that in the region of small quark masses, which

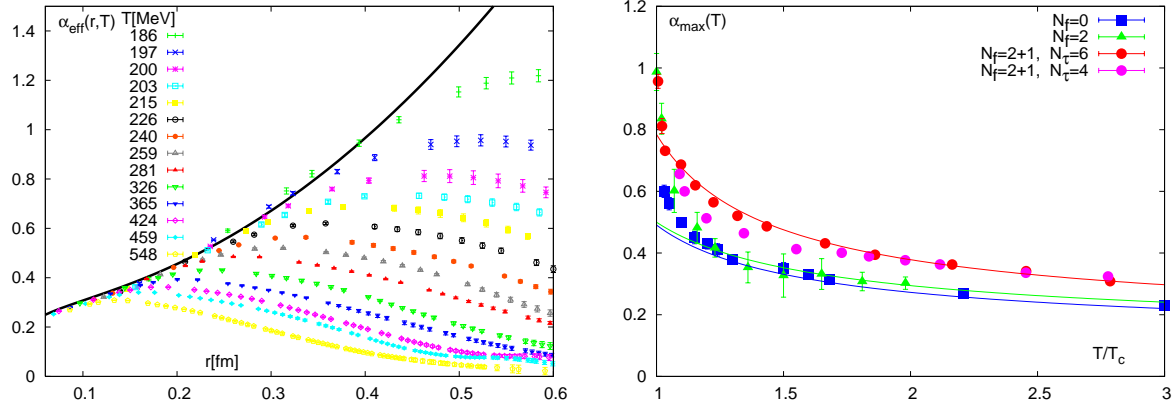


**Figure 3:** Temperature dependence of the effective running coupling at various values of the temperature (left). The black solid line shows the result at zero temperature. The right hand figure shows the maximal value attained by  $\alpha_{\text{eff}}(r, T)$  in calculations of QCD with different flavor content.

has been studied by us, the flavor and quark mass dependence of the deconfinement transition can be almost entirely understood in terms of the flavor and quark mass dependence of the transition temperature  $T_c$ . We note that a similar renormalization procedure of the Polyakov loop as discussed above was also used in Ref. [17]. We also note that in Ref. [17] a different normalization convention for the zero temperature potential has been used and therefore the absolute value of the Polyakov loop is quite different.

#### 4. Running Coupling

Now let us discuss our results on the distance and temperature dependence of the singlet free energies in terms of a running coupling constant. We define the temperature-dependent coupling analogously to the zero temperature case through the free energy,

$$\alpha_{\text{eff}}(r, T) = \frac{3}{4} r^2 \frac{dF_1(r, T)}{dr}. \quad (4.1)$$

In Fig.3 (left) we present our results for the running coupling. At short distances, especially at low temperatures, it coincides with the zero temperature coupling until screening sets in. After reaching a maximal value it decreases slowly. At higher temperature the shift of the maximum to shorter and shorter distances again indicates that screening effects set in at shorter distances. However still the running coupling rises quadratically at intermediate distances, before screening sets in. This arises from the linear confinement part of the static potential and signals the remnants of confining forces even at rather high temperatures. We, therefore, can conclude that remnants of the confining force still are important for physics at moderately large distances even in the high temperature phase of QCD. The maximal value of the effective running coupling along with fits inspired by a perturbative Ansatz are shown in the right hand part of Fig. 3. One can see that the maximal value decreases only slowly with temperature and even at three times the transition temperatures it is only a factor five smaller than at the transition temperature. For comparison we show here also results obtained in simulations of 2-flavor QCD with larger quark mass ( $m/T = 0.4$ ) and

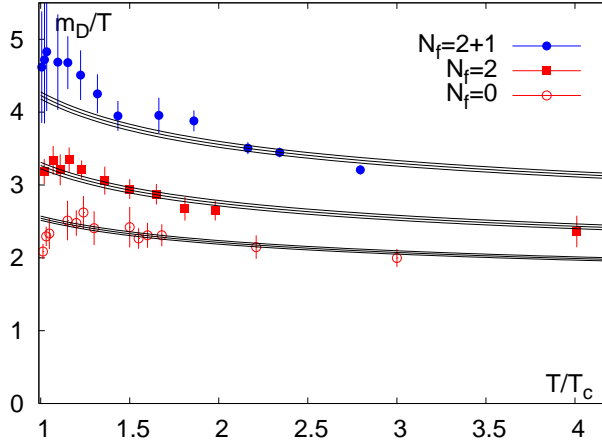


**Figure 4:** Screening masses in  $(2+1)$ -flavor QCD versus temperature. For comparison results from calculations in 2-flavor QCD and pure gauge theory are included. Lines represent fits to leading order perturbation theory with free pre-factor  $A$ .

pure gauge theory results. The large value of the effective coupling is again due to the linearly rising term in the potential. As one can see from the comparison of results obtained for two different lattice spacings, cut-off effects for the effective coupling are small.

## 5. Screening masses

To analyze the exponential screening of free energies at large distances we extract screening masses. They are determined from fits to the large distance part of the free energy where we subtracted the asymptotic cluster value,

$$F_1(r, T) - F_1(r = \infty, T) = -\frac{4}{3} \frac{\alpha(T)}{r} \exp(-m_D(T)r) . \quad (5.1)$$

To leading order in perturbation theory the screening (Debye) mass is given by

$$\frac{m_D}{T} = A \left( 1 + \frac{N_f}{6} \right)^{1/2} g(T) . \quad (5.2)$$

In Fig.4 we show screening masses as function of temperature. In addition to results from our  $(2+1)$ -flavor simulations we also show results from calculations performed in 2-flavor QCD and pure gauge theory. These numerical results are compared to leading order perturbation theory, where we allow for a pre-factor  $A$  which is fixed by a fit to the data. This pre-factor is slightly different for each case. We can see, however, that the temperature dependence of the screening masses in all cases is described quite well by the perturbative Ansatz.

## 6. Conclusions

We have significantly expanded our analysis of heavy-quark related physics through large scale simulations in  $(2+1)$ -flavor QCD. The renormalized Polyakov loop shows little cut-off dependence

and can be calculated reliably on relatively coarse lattices. We find that its flavor and quark mass dependence can be absorbed almost entirely in the flavor and quark mass dependence of the transition temperature. The analysis of screening masses shows that non-perturbative effects can be well absorbed in a pre-factor in front of the leading order perturbative result which is temperature independent in the entire temperature range analyzed here. This indicates that the true perturbative limit, corresponding to  $A \equiv 1$ , is approached only very slowly.

The temperature dependent effective running coupling constant rises quadratically at moderate distances also above the transition temperature. After reaching a maximal value that is reached at smaller distances with increasing temperature it drops exponentially. Also this maximal value decreases only slowly with temperature.

## References

- [1] L.D. McLerran, B. Svetitsky, *Phys. Rev. D* **24** (1981) 450
- [2] T. Matsui and H. Satz, *Phys. Lett. B* **178** (1986) 416
- [3] A. Jakovác, P. Petreczky, K. Petrov and A. Velytsky, *Phys. Rev. D* **75** (2007) 014506
- [4] S. Digal, P. Petreczky and H. Satz, *Phys. Lett. B* **514** (2001) 57; *Phys. Rev. D* **64** (2001) 094015
- [5] Á. Mócsy and P. Petreczky, *Phys. Rev. D* **73** (2006) 074007; arXiv:0705.2559 [hep-ph]; arXiv:0706.2183 [hep-ph].
- [6] M. Cheng *et al.*, arXiv:0710.0354 [hep-lat].
- [7] A. Gray *et al.*, *Phys. Rev. D* **72** (2005) 094507 (
- [8] M. Cheng *et al.*, *Phys. Rev. D* **74** (2006) 054507
- [9] O. Philipsen, *Phys. Lett. B* **535** (2002) 138
- [10] O. Kaczmarek, F. Karsch, P. Petreczky and F. Zantow, *Phys. Lett. B* **543** (2002) 41
- [11] S. Digal, S. Fortunato and P. Petreczky, *Phys. Rev. D* **68** (2003) 034008
- [12] O. Kaczmarek, F. Karsch, F. Zantow and P. Petreczky, *Phys. Rev. D* **70** (2004) 074505
- [13] P. Petreczky and K. Petrov, *Phys. Rev. D* **70** (2004) 054503
- [14] O. Kaczmarek and F. Zantow, *Phys. Rev. D* **71** (2005) 114510; arXiv:hep-lat/0506019; O.Kaczmarek *et al. Prog.Theor.Phys.Suppl.* **153** (2004) 287
- [15] C. Aubin *et al.*, *Phys. Rev. D* **70** (2004) 094505
- [16] C. Bernard *et al.* [MILC Collaboration], *Phys. Rev. D* **71** (2005) 034504
- [17] Y. Aoki, Z. Fodor, S. D. Katz and K. K. Szabo, *Phys. Lett. B* **643** (2006) 46
- [18] K. Petrov [the RBC-Bielefeld Collaboration], *PoS LAT2006* (2006) 144